JOURNAL OF MATERIALS SCIENCE 26 (1991) 4394–4398

Fracture toughness measurement with fatigue-precracked single edge-notched beam specimens of WC-Co hard metal

H. IIZUKA, M. TANAKA
Mining College, Akita University, Tegatagakuen-cho 1-1, Akita 010, Japan

The plain-strain fracture toughness of WC–8%Co hard metal, K_{IC}, was measured using single edge-notched beam (SENB) specimens with fatigue precrack. The fatigue precrack was introduced with compressive fatigue cycling in four-point bending at room temperature. Since stable fatigue-crack propagation was obtained from the notch tip, it was easy to control the fatigue-precrack length. A reasonable K_{IC} value of 13.3 MPa $m^{1/2}$ was obtained with the fatigue-precracked SENB specimens in four-point bending. The compressive fatigue-precracking technique in four-point bending was simple and convenient, and is therefore applicable to precracking in a variety of brittle materials prior to fracture-toughness measurements.

1. Introduction

The plain-strain fracture-toughness parameter, K_{IC}, has been determined using a variety of different specimen geometries such as the single edge-notched beam (SENB) specimen, the double cantilever beam specimen, the double torsion specimen, the short rod/bar specimen and the chevron notched specimen [1, 2]. The main difficulties in K_{IC} determination with SENB specimens are the introduction of a sharp precrack, and the measurement of its length when this can be successfully introduced. Economical specimen preparation is also necessary. Several methods have been advocated in the past, however no single method has gained wide acceptance. Mechanical precracking by the usual methods of fatigue cycling or wedge loading is difficult because the necessary stress-intensity factor for precracking is often very close to the critical fracture toughness in hard metals and ceramics. Special techniques are therefore needed for precracking in these materials.

The bridge compression [3] and cyclic loading [4–7] methods are promising, since these methods can introduce an ideal sharp precrack. However, they do have some limitations and should be investigated thoroughly for wider application. For example, there is a difficulty in the reproduction of bridge-compression precracks of the same size. Residual stresses resulting from the bridge-compression precracking procedure affect the measured fracture toughness [3]. The high-temperature fatigue precracking procedure may produce crack closure resulting from the formation of an oxide film on the fracture surface [4]. Moreover, it is known that the precrack length in compressive fatigue cycling is limited to the size of the local damage zone at the notch root [5]. Suresh and co-workers [6, 7] showed that crack propagation under uniaxial cyclic compression offers a novel possibility for precracking in brittle materials prior to fracture-toughness measurements.

In this paper, compressive fatigue crack propagation from the notch-tip was observed in four-point bending specimens at room temperature. Fracture toughness, K_{IC}, was measured with fatigue-precracked SENB specimens. Discussion was made on the possibility of compressive bending-fatigue cycling for the precracking prior to fracture-toughness measurement.

2. Experimental procedure

The material used was WC–8%Co hard metal, the average grain diameter of the WC particles being about 2.1 μm. The fracture strength was 2.3 GPa. The size of the SENB specimen was $3 \times 6 \times 60$ mm. Notches were introduced by spark cutting with an electrical-discharge machine. The notch depth, d, was 1.5 mm, notch width was 0.27 mm and the notch-root radius, ρ, was 0.14 mm.

Fatigue precrackings and fracture-toughness tests were carried out using servocontrolled fatigue-test equipment at room temperature. Fig. 1 shows diagrams of SENB specimens subjected to compressive fatigue cycling for precracking and loading for fracture-toughness tests in four-point bending, in which the outer span, L_1, was 50 mm and the inner span, L_2, was 10 mm. Fully compressive cyclic loads of a triangular wave-shape (5 Hz frequency) were applied at room temperature for precracking. The maximum load, P_{max}, was 2.5–3.5 kN, which corresponded to 1.4–2.0 GPa in tensile stress at the smooth specimen surface. The load ratio, $R = P_{min}/P_{max}$, was maintained at a constant value of 0.1 in all experiments.

0022–2461/91 $03.00 + .12

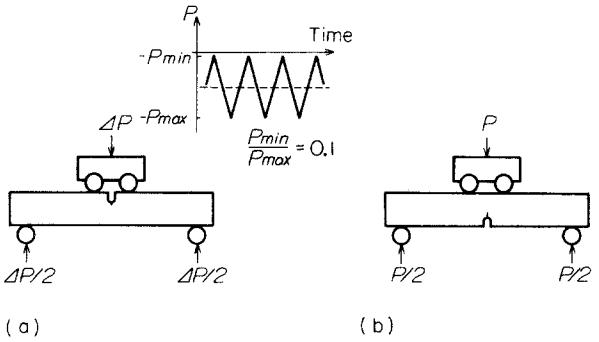

Figure 1 Schematic diagram of SENB specimen subjected to (a) compressive fatigue cycling for precracking and (b) tensile loading for fracture-toughness tests in four-point bending.

The cross-head speed was 2.1×10^{-3} mm sec^{-1} in fracture-toughness tests.

K_{IC} was also measured with the indentation-fracture method [8, 9] and the natural-flaw method [2]. The indentation-fracture method was carried out with a Vickers hardness tester: the indentation load was 490 N and the hold time 30 sec. Measurements were performed after surface polishing of about 60 μm with diamond paste. In the natural-flaw method, K_{IC} was calculated with the largest natural flaw which was observed on the fracture surfaces in fracture-strength tests with four-point bending. The K_{IC} values obtained are listed in Table I.

The stress-intensity factor, K, of the fatigue precrack which was initiated at the notch-tip was calculated with [10]

$$K = Y \cdot 3P(L_1 - L_2)a^{1/2}/(2bW^2) \quad (1)$$

where P is the applied load, a is the total crack length, b is the specimen width, W is the specimen height, and Y is the modification factor which is calculated by

$$Y = 1.99 - 2.47(a/W) + 12.97(a/W)^2 - 23.17(a/W)^3 + 24.80(a/W)^4 \quad (2)$$

3. Results and discussion

3.1. Introduction of compressive fatigue precrack

Fig. 2 shows the influence of compressive fatigue cycling on fatigue-crack propagation from the notch tip. Stable crack propagation was produced under all loading conditions. It is known that the important contribution to such crack initiation and propagation arises from the residual tensile stresses induced locally at the notch tip [6, 7]. The fatigue cracks propagate at a progressively decreasing velocity until the cracks are arrested completely. The final crack length was longer, with larger values of P_{max}. However, extremely large load amplitude resulted in catastrophic failure from the tensile-stress side of the specimens. It was difficult to introduce a precrack longer than about 0.13 mm in WC–8%Co with this specimen geometry.

The crack-arrest distance under compressive fatigue is dictated by the competing effects of the residual tensile-stress field and the development of crack closure with an increase in crack length [7]. To obtain longer precracks, the contact portions in the wake of the fatigue crack were removed with aqua-regia etching. After etching, the arrested cracks were re-started: Fig. 3 shows the re-started crack propagation. The crack-propagation rate was also progressively reduced until it was re-arrested. Fig. 4 shows the arrested fatigue precrack and the re-started fatigue precrack. The re-started fatigue crack also had a sharp crack tip.

Fig. 5 shows the fatigue-precrack profile on fracture surface. Slight non-uniformity in the fatigue-crack front occurred during fatigue cycling. The crack propagation distance within about 0.5 mm of the side surfaces was larger than that in the interior of the secimen, l_i. l_s was 0.01–0.03 mm longer than l_i when l_i = 0.07–0.22 mm, where l_s is the crack propagation distance at the side surface. The effect of this crack-tip profile on the K_{IC} measurements is considered to be small, since the ratio of $(d + l_i)$ to $(d + l_s)$ was higher than 0.95, where d is the notch depth. Ewart and Suresh [6] observed a similar crack profile under uniaxial compressive fatigue in Al_2O_3.

3.2. Fracture toughness

Fig. 6 shows the effect of fatigue-precrack propagation distance, l_i, on the necessary stress-intensity factor for crack extension, K_{IR}. K_{IR} was decreased with the increase of l_i, and was approximately constant when l_i was longer than about 0.09 mm. The average value of K_{IR} was 13.3 MPa m$^{1/2}$ under $l_i > 0.09$ mm.

TABLE I Results of fracture-toughness tests on WC–8%Co

Method	Results			
	Surface flaw depth (μm)	Circular pore diameter (μm)	K_{IC} (MPa m$^{1/2}$)	σ (MPa m$^{1/2}$)
Indentation flaw	–	–	14.25[a]	0.56
Natural flaw	8	–	12.31[b]	–
	34	–	13.49[b]	–
	–	29	13.86[c]	–
	–	20	12.80[c]	–

[a] $K_{IC} = 0.011\, E^{0.4} P^{0.6} a^{-0.7} (l/a)^{-0.5}$ where E = Young's modulus; P = applied load; a = diagonal length of indentation; l = Palmquvist-crack length, from [10].
[b] K_{IC} calculated with equation in [11].
[c] K_{IC} calculated with equation in [12].

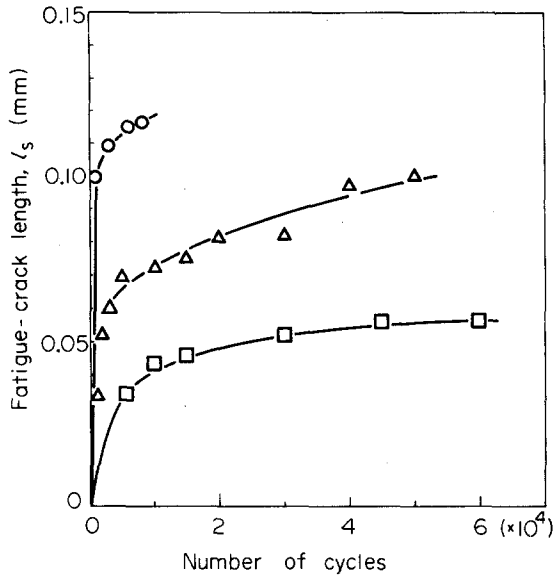

Figure 2 Influence of compressive cycling on fatigue crack propagation. P_{max} = ○, 3.5; △, 3.1; □, 2.9 kN.

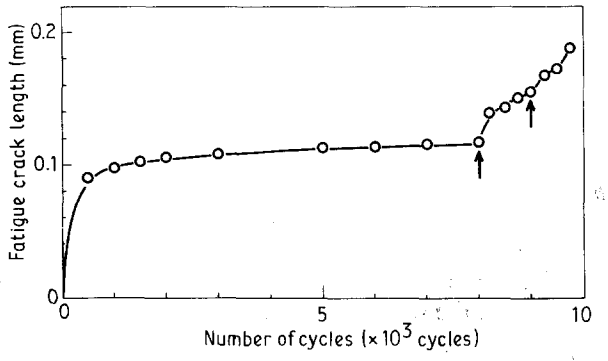

Figure 3 Effect of aqua-regia etching on re-start of arrested fatigue crack. Arrow indicates the point of time when the fracture surface was etched with aqua-regia. P_{max} = 3.5 kN.

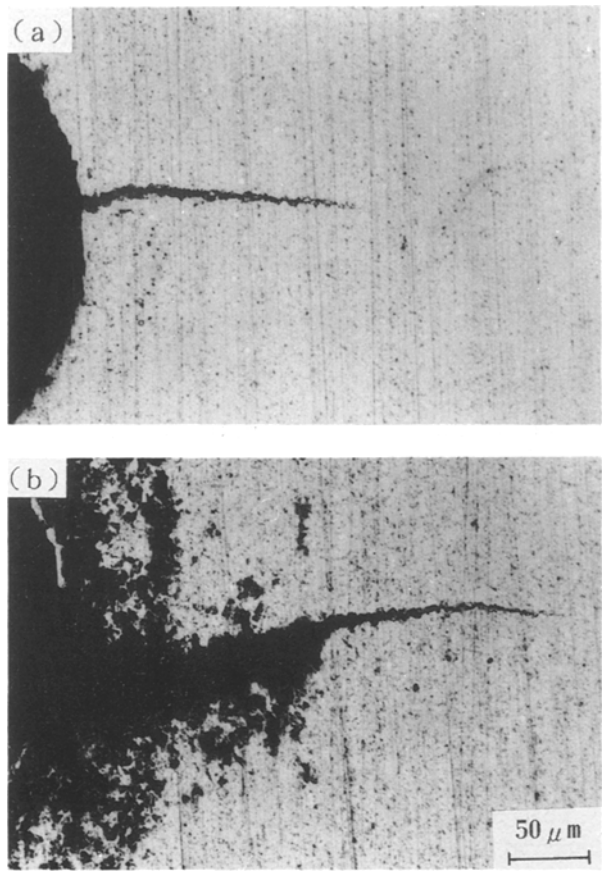

Figure 4 Fatigue precrack. (a) P_{max} = 3.5 kN; (b) fatigue precrack re-started after aqua-regia etching, P_{max} = 3.5 kN.

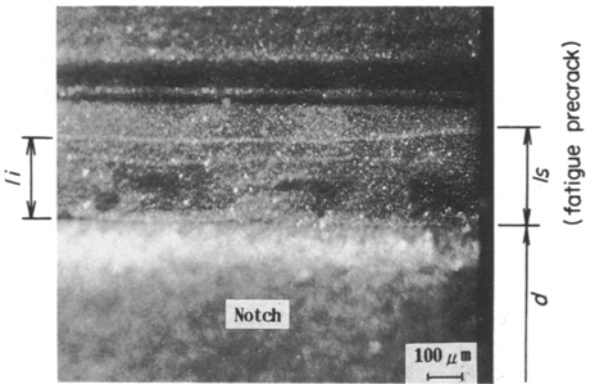

Figure 5 Fatigue precrack profile on fracture surface. P_{max} = 2.9 kN.

The extent of scatter in the results was small. Moreover, the average values obtained were almost equal to the K_{IC} values which were obtained with the natural-flaw and indentation-fracture methods. Therefore it is considered that reasonable K_{IC} values were obtained when l_i was longer than about 0.09 mm. The re-started fatigue precracks in the aqua-regia etched specimens were extended further than about 30 WC grains after last etching, prior to fracture-toughness tests.

The influence of notch geometry on the stress-intensity factor, K, of the precrack which was initiated at the notch tip was analysed by Nishitani and co-workers [13, 14]. The value K of the precrack was strongly influenced by ρ/d. However, K of the precrack is almost equal to that of the through-thickness crack with the same total crack length when ρ/d is small. For example, according to Nishitani and Ishida [14], $K/\sigma[\pi(d + l_i)]^{1/2} = 1.11$ for $\rho/d = 0.125$ and $l_i/d = 0.1$. These results show that one can calculate K of the precrack regardless of the influence of notch geometry when ρ/d is small. In this study, ρ/d is 0.1 and $l_i/d = 0.1$ when $l_i = 0.15$ mm. Therefore the influence of notch geometry on the calculation of K of the precrack with Equation 1 seems to be small when $l_i = 0.15$ mm. The results shown in Fig. 6 indicate that the influence of the notch geometry is small when l_i is larger than about 0.09 mm. The slightly higher K_{IR} values when l_i is smaller than 0.09 mm are explained by the fact that the K values calculated with Equation 1 were larger than the real driving force, K.

K_{IR} measured with the notched specimen ($l_i = 0$) was about 60% higher than 13.3 MPa m$^{1/2}$. Higher K_{IR} values were obtained in notched specimens with larger notch-root radii in many brittle materials. For example, $\rho > 70$ μm in Al_2O_3 with 10 μm grain size [15], $\rho > 60$ μm in Al_2O_3 with 10 μm grain size [16], and $\rho > 10$ μm in Si_3N_4 and SiC with 3–4 μm grain size [16]. It is known that K_{IR} values measured with

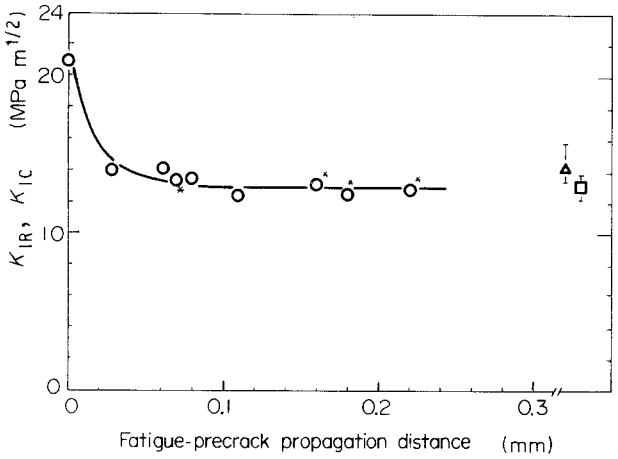

Figure 6 Effect of fatigue-precrack propagation distance, l_i, on necessary stress-intensity factor for crack extension, K_{IR}. *, Results measured with aqua-regia etched specimens. K_{IC} measured with Δ, indentation-flaw method; □, natural-flaw method.

notched specimens are proportional to the square root of the notch radius, ρ, for ρ greater than a limiting sharpness [15, 16]. The critical notch radius to obtain a reasonable K_{IC} is strongly influenced by the grain size [16].

In general, the effect of residual stress produced in precracking on measured toughness values is important. However, the maximum extent of damage left at the crack tip under compressive fatigue cycling is not likely to affect subsequent fracture-toughness measurements. This assumption has been experimentally substantiated in metal under far-field uniaxial compressive load [6].

3.3. Microstructural observations

Fig. 7 shows the difference between the fatigue-fracture surface and the catastrophic bend-fracture surface produced in fracture-toughness tests. The most notable difference was the amount of plastic deformation in cobalt ligaments, which were strongly deformed and ruptured on the bend-fracture surfaces. On the fatigue-fracture surfaces, large plastic deformation of cobalt ligaments was not observed. Therefore it was easy to measure the fatigue-precrack propagation distance on the fracture surfaces. Moreover, it was confirmed that the aqua-regia etching had no influence on the features of the bend-fracture surfaces.

Suresh and co-workers [6, 7] found that the crack-propagation rate was progressively reduced until it was arrested under far-field uniaxial cyclic compression in metals and brittle materials, and emphasized that this phenomenon has some important applications as a sharp precracking technique for fracture-toughness measurements in brittle materials. The results obtained in this study also show that compressive fatigue precracking is useful in brittle materials. Moreover, the compressive fatigue-precracking technique in four-point bending is simple and convenient. The extent of maximum load for precracking is lower in four-point bending than in uniaxial cyclic compression [7] or in bridge compression [3]. Therefore, this method is applicable to precracking in a variety of brittle materials prior to fracture-toughness measurements.

4. Conclusions

The fracture toughness value, K_{IC}, of WC–8%Co, was measured with SENB specimens with fatigue precracks. The fatigue precracks were introduced by compressive fatigue cycling in four-point bending. The results obtained were as follows:

1. A reasonable K_{IC} value of 13.3 MPa m$^{1/2}$ was obtained with fatigue-precracked SENB specimens when the fatigue-precrack propagation distance was larger than about 0.09 mm from the notch tip at which the notch-root radius was 0.14 mm.
2. The compressive fatigue precracking technique was simple and convenient, since the stable crack propagation was obtained in compressive fatigue cycling. This method is applicable to precracking in a variety of brittle materials prior to fracture-toughness measurements.

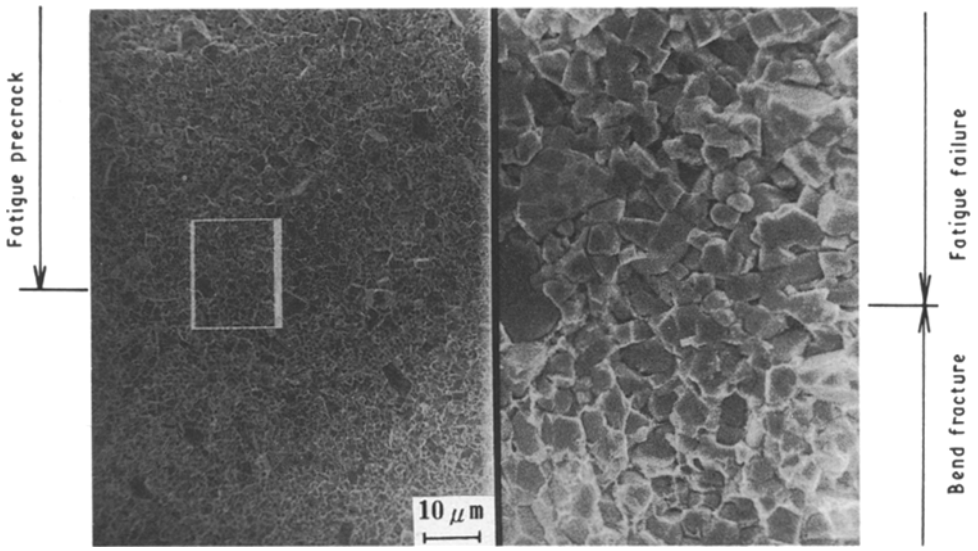

Figure 7 Scanning electron micrographs. Fatigue-fracture surface produced with P_{max} = 2.5 kN.

Acknowledgements

The authors gratefully acknowledge the experimental work of K. Morokoshi, graduate of Akita University, and the specimen preparation by Kobayashi Industry Co. Ltd, Akita, Japan.

References

1. D. MUNZ, in "Fracture Mechanics of Ceramics", edited by R. C. Bradt *et al.* (Plenum, New York, 1983) p. 1.
2. S. W. FREIMAN, *ibid.* p. 27.
3. R. GODSE, J. GURLAND and S. SURESH, *Mater. Sci. Engng* **A105/106** (1988) 383.
4. Y. MUTOH, K. TANAKA, T. NIWA and N. MIYAHARA, *J. Mater. Sci.* **23** (1988) 3939.
5. S. SURESH, L. EWART, M. MADEN, W. S. SLAUGHTER and M. NGUYEN, *ibid.* **22** (1987) 1271.
6. L. EWART and S. SURESH, *ibid.* **22** (1987) 1173.
7. S. SURESH and J. R. BROCKKENBROUGH, *Acta Metall.* **36** (1988) 1455.
8. M. T. LAUGER, *J. Mater. Sci.* **6** (1987) 897.
9. G. R. ANSTIS, P. CHANTIKUL, B. R. LAWN and D. B. MARSHALL, *J. Amer. Ceram. Soc.* **64** (1981) 533.
10. T. NISHIDA and E. YASUDA, in "Evaluation of Mechanical Properties in Ceramics" (in Japanese), (Nikkan-kougyo-shinbunsha, Tokyo, 1986) p. 83.
11. M. ISHIDA and H. NOGUCHI, *Trans. Jpn Soc. Mech. Engng* **48** (1982) 607 (in Japanese).
12. F. W. SMITH, A. S. KOBAYASHI and A. F. EMERY, *Trans. ASME, Ser. E* **89** (1967) 947.
13. H. NISHITANI and M. ISHIDA, *Trans. Jpn Soc. Mech. Engng* **39** (1973) 7 (in Japanese).
14. H. NISHITANI and Y. ODA, *ibid.* **46** (1980) 745 (in Japanese).
15. R. L. BERTOLOTTI, *J. Amer. Ceram. Soc.* **56** (1973) 107.
16. I. TAKAHASHI, S. USAMI, K. NAKAKADO, H. MIYATA and S. SHIDA, *Yogyo-Kyokai-Shi* **93** (1985) 186 (in Japanese).

Received 26 March
and accepted 20 December 1990